Disc iminating etween Input Signals Via Single Neu on Activity

Jianfeng Feng*,** Feng Liu*,***

*COGS, University of Sussex at Brighton, BN1 9QH, UK

**Newton Institute, Cambridge University, CB3 0EH, UK

*** Department of Physics, Nanjing University, Nanjing 210093, P.R.China

jianfeng@cogs.susx.ac.uk http://www.cogs.susx.ac.uk/users/jianfeng

Abstract

What is neuronal capability of discriminating between different input signals? Furthermore, how to improve its discriminating capability? We explore these issues both theoretically and numerically for the integrate-and-fire (IF) model and the IF-FHN model (a simplified version of the FitzHugh-Nagumo model [6]). It is found that adding correlations and increasing inhibitory inputs considerably reduce the total probability of misclassifications (TPM). A novel theory on discrimination tasks is developed and the theory accounts for all observed numerical results.

1 Introduction

To efficiently discriminate between different input signals, for example to tell the image of a prey from that of a predator, is of vital importance to a nervous system. The actual

that the information extracted from single neuron activity in MT is almost enough to account for psychophysical experiment data. Hence an observation of the firing rates of single neuron, at least in MT, contains enough information to further guide motor activity. Imagining the enormous number of neurons in the cortex, their findings are striking and open up many interesting issues for further theoretical and experimental study. Interestingly, similar findings are reported in somatosensory pathways [15] as well. In line with these experimental results, in this paper we concentrate on the relationship of the input and output firing rates of a single neuron. The issue we are going to address is quite straightforward (see Fig. 1). Suppose that a neuron receives two set

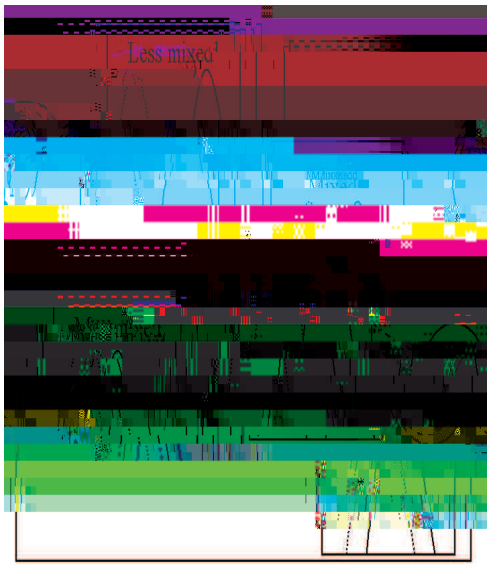

Figure 1: For two mixed signals (left), after

ed?

oy firing rates) distributed according to two his

gnals become more mixed or

fire(IF) model and the IF-FHN

Theoretically the critical value of the coherent inputs at which the output histograms are separable is exactly obtained (Theorem 2) for the case of correlated and exactly balanced inputs (the most interesting case). The results enable us to assess the dependence of our conclusions on different model parameters and input signals. It is illuminating to see that the critical value is independent of model parameters including the threshold, the decay time and the EPSP and IPSP magnitude.

All the aforementioned results are obtained for the IF and IF-FHN model without reversal potentials, we further examine our conclusions for the IF model with reversal potentials. Since adding reversal potentials to a model is equivalent to increasing its decay rate (depending on input signals), we would naturally expect that the model with reversal potentials will become more effectively to distinguish different inputs. The conclusion is numerically confirmed.

During the past few years, inhibitory inputs (see for example [11, 12]) and correlated inputs (see for example [17, 18] are two topics widely investigated in neuroscience. It seems it is generally accepted that they play important roles in information processing in the brain. Our results here provide a convincing and direct evidence to show that they do improve the performance of a single neuron. Such results would also be valuable on practical applications of spiking neural networks [9].

2 The Integrate-and-fire Model and its Inputs

The first neuron model we use here is the classical Ed[(enest)Tj23.4184tions

with E_i

correlation coefficient between ith excitatory (inhibitory) synapse and jth excitatory (inhibitory) synapse is $c \geq 0$. The correlation considered here reflects the correlation of activity of different synapses, as discussed and explored in [6, 21]. It is not the correlation of single incoming EPSP or IPSP which could be expressed as $c_{ij}(t-t')$ for the EPSP (IPSP) at time t of the ith synapse and time t' of the jth synapse. We refer the reader to [6] for a detailed discussion on the meaning of the correlation considered here.

In summary, suppose that a neuron receives p synaptic inputs. The goal of the postsynaptic neuron is to discriminate between two types of inputs

1. p_c excitatory

direction of a dot. Denote that $N_i(t), i = 1, \cdots, p$ as a Poisson process with a rate ζ_i, where ζ_i takes value from $[0, 100]$Hz, i.e. $(\zeta_i/$

about 13.5% and for the right upper panel is 5.5%. Therefore adding inhibitory inputs to the neuron considerably improves its discrimination capability, reducing TPM from 13.5% to 5.5%.

In Fig. 4 the histogram of coefficient of variation (CV) of efferent spike trains is plotted. Our results also reveal one possible functional role of efferent spike trains with a high CV widely observed in experiments. In the past few years, there are a large body of literatures devoted to the topic: how to generate efferent spike trains with a large CV for the IF model(see [6] for a review). Nevertheless, the functional implications of efferent spike trains with a large CV are still not clear. Here we find that for a fixed coherence level, a lower TPM value corresponds to a larger exp discriminam9840Td1f7ds :

than harmful. The benefit of noise in neuronal system has been extensively explored in the literature of stochastic resonance [8]. However, the mechanism to reach the finely tuning noise level which results in the stochastic resonance seems far-fetched for neuronal systems. Our finding here provides a more direct and convincing evidence which clearly demonstrates the advantage of adding noise to a neuronal system.

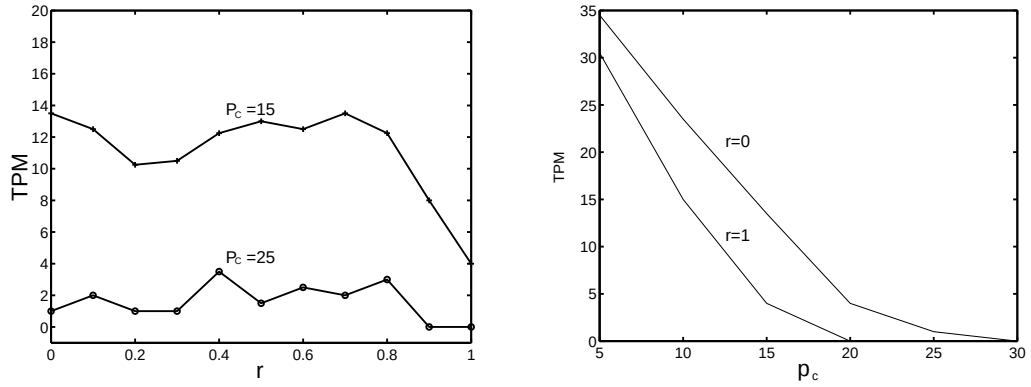

Figure 5: TPM vs. r (left) and TPM vs. p_c (right) for the IF model. When $p_c = 15$ (left), it is clearly shown that TPM attains its optimal value at $r = 1$,

The input in the previous subsection is

$$\begin{aligned} di_{syn}(t) &= a(p_c\lambda_j + \sum_{i=1}^{p-p_c}\xi_i)(1-r)dt \\ &\quad + a\sqrt{[\lambda_j p_c(1+c(p_c-1)) + \sum_{i=1}^{p-p_c}\xi_i](1+r)}\cdot dB_t \\ &= \mu dt + \sigma dB_t \end{aligned} \tag{3.1}$$

where $j = 1, 2$. From results in [6] we know that

$$\langle T\rangle = \frac{2}{L}\int_{\frac{V_{rest}L-\mu}{\sigma}}^{\frac{V_{thre}L-\mu}{\sigma}} g(x)dx \tag{3.2}$$

where

$$g(x) = \left[\exp(x^2)\int_{-\infty}^{x}\exp(-u^2)du\right]$$

In terms of the law of large numbers we conclude that

$$\sum_{i=1}^{p-p_c}\xi_i \sim (p-p_c)\langle\xi_1\rangle + \sqrt{p-p_c}\xi\sigma(\xi_1) \tag{3.3}$$

where $\sigma(\xi_1)$ is the standard deviation of ξ_1 and $\xi \sim N(0,1)$.

Hence Eq. (3.2) turns out to be

$$\begin{aligned} \langle T\rangle = \frac{2}{L} & \\ \cdot \int_{\frac{V_{thre}L - a[p_c\lambda_j + (p-p_c)\langle\xi_1\rangle + \sqrt{p-p_c}\xi\sigma(\xi_1)](1-r)}{a\sqrt{[\lambda_j p_c(1+c(p_c-1)) + (p-p_c)\langle\xi_1\rangle + \sqrt{p-p_c}\xi\sigma(\xi_1)](1+r)}}}^{\frac{-[p_c\lambda_j + (p-p_c)\langle\xi_1\rangle + \sqrt{p-p_c}\xi\sigma(\xi_1)](1-r)}{\sqrt{[\lambda_j p_c(1+c(p_c-1)) + (p-p_c)\langle\xi_1\rangle + \sqrt{p-p_c}\xi\sigma(\xi_1)](1+r)}}} & g(x)dx \end{aligned} \tag{3.4}$$

We have checked the accuracy of the approximation developed here. It is found that the approximation in Eq. (3.4) is not very good (compare Fig. 6 upper panel with Fig. 3 upper panel), simply implying that we have to include more higher order terms in the approximation of wt9esspp elbpre d It isinr/W1/-351.68023.40Td[Tjrm.08010ula

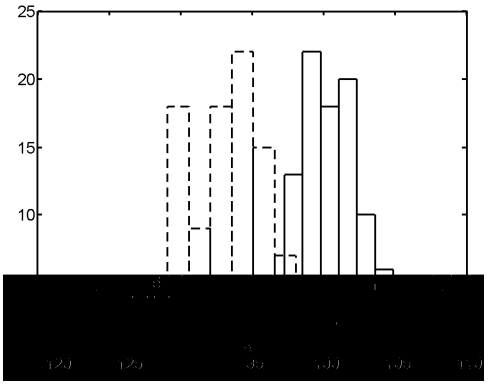
25
20
15
10

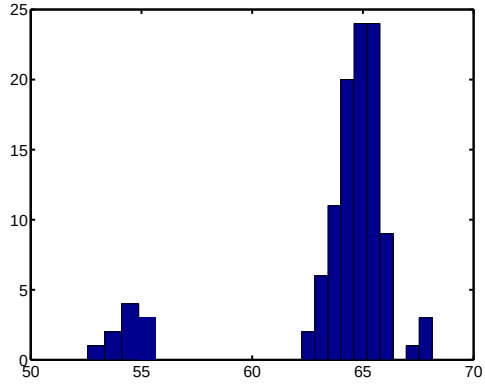
25
20
15
10
5
0
50
55
60
65
70

To the first order approximation, Eq. (3.4) reveals the underpinning mechanism of the phenomena observed here. From Eq. (3.4) we have

$$\langle T\rangle \sim \langle T_1\rangle = \frac{2g(0)V_{thre}}{a\sqrt{[\lambda_j p_c(1+c(p_c-1))+(p-p_c)\langle\xi_1\rangle+\sqrt{p-p_c}\xi\sigma(\xi_1)](1+r)}} \tag{3.5}$$

The firing rate in the unit of Hz is then

$$= \frac{\frac{1000}{R_e+\langle T_1\rangle}}{1000a\sqrt{[\lambda_j}}$$

$\sigma(\xi_1) = .1/\sqrt{12}$ (upper panel) and $\sigma(\xi_1) = 1/\sqrt{12}$ (bottom panel). When $\langle\xi_1\rangle = 0.05$ and $\sigma(\xi_1) = .1/\sqrt{12}$, the mean and variance are the same as in the model considered in the previous subsections. When $\langle\xi_1\rangle = 0.05$ and $\sigma(\xi_1) = 1/\sqrt{12}$, the standard deviation of inputs is enlarged by a factor of 10, in comparison with the setup in the previous subsections. It is easily seen that increasing the variance in input signals will make the histograms of firing rates more widely spread out, as shown in Fig. 6, bottom panel. Nevertheless, when $p_c = 25$ we see that the input signals can be perfectly separated.

3.2 Models With Reversal Potentials

A slightly more general model than the IF model defined above is the IF model with reversal potentials defined by

$$dZ_t = -(Z_t - V_{rest})Ldt + d\bar{I}_{syn}(Z_t, t) \tag{3.9}$$

where

$$\bar{I}_{syn}(Z_t, t) = \bar{a}(V_E - Z_t)\sum_{i=1}^{p} E_i(t) + \bar{b}(V_I - Z_t)\sum_{j=1}^{q} I_j(t)$$

V_E and V_I are the reversal potentials $V_I < V_{rest} < V_E$, $\bar{a}(V_E - V_{rest}), \bar{b}(V_I - V_{rest})$ are the magnitude of single EPSP and IPSP when $Z_t = V_{rest}$. We could rewrite Eq. (3.9) in the following form

$$\begin{aligned} dZ_t &= -(Z_t - V_{rest})(Ldt + \bar{a}\sum_{i=1}^{p} dE_i(t) + \bar{a}\sum_{i=1}^{p} dI_i(t)) \\ &\quad +\bar{a}(V_E - V_{rest})\sum_{i=1}^{p} dE_i(t) + \bar{b}(V_I - V_{rest})\sum_{j=1}^{q} dI_j(t) \\ &= -(Z_t - V_{rest})[Ldt + \bar{a}\sum_{i=1}^{p} dE_i(t) + \bar{b}\sum_{i=1}^{p} dI_i(t)] \\ &\quad +a\sum_{i=1}^{p} dE_i(t) + b\sum_{j=1}^{q} dI_j(t) \end{aligned} \tag{3.10}$$

Therefore the difference between the model with and without reversal potentials is that the latter has a decay rate depending on incoming signals. From

the previous subsections we would expect that the model with reversal potentials will improve its capacity of discriminating incoming signals.

Fig. 7 is in agreement with our expectations. We see that for $p_c = 15$ and $r = 0.6$ a perfect discrimination is achieved. For the model without reversal potentials, we see that for $p_c = 15$ and $r = 1$ we still have TPM $\blacksquare$ 0 (see previous subsections). The parameters used in the model with reversal potentials are $\bar{a} = 0.01, \bar{b} = 0.1, V_E = 100mV, V_I = -10mV$, with all other parameters as the model without reversal potentials.

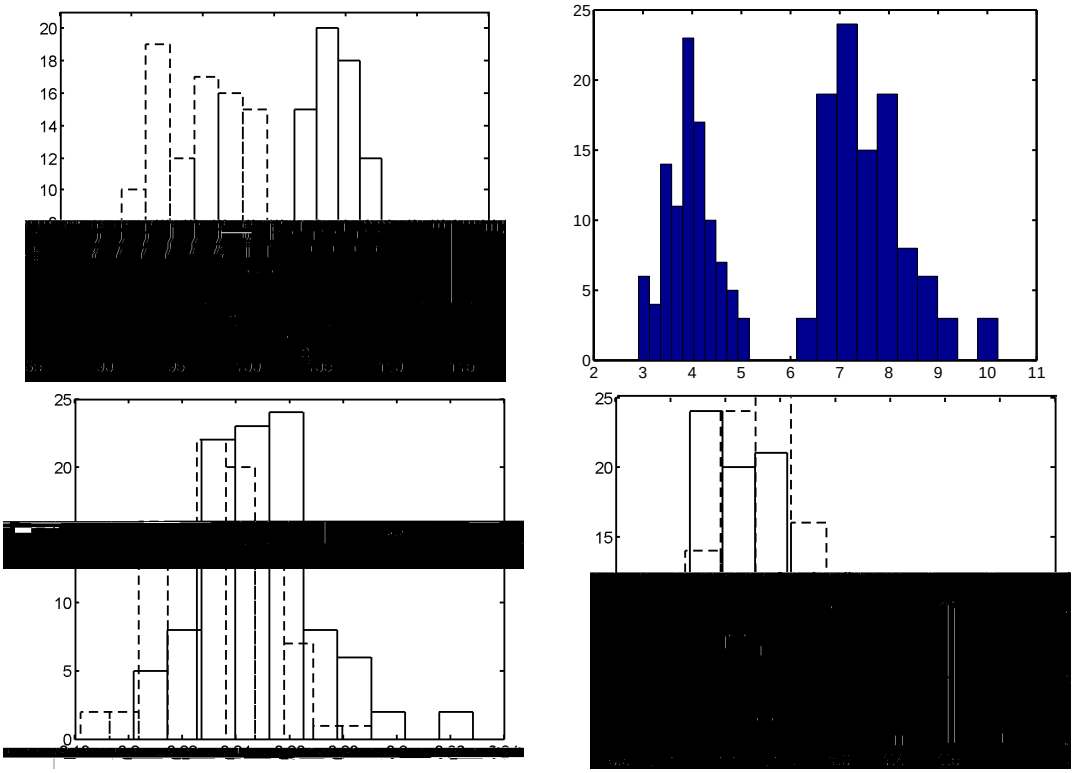

Figure 7: Histogram of firing rates in the unit of Hz (upper panel) and CV (bottom panel) with $c = 0.1, p_c = 15$ for the IF model with reversal potentials. Left, exclusively excitatory inputs $r = 0$. Right, $r = 0.6$.

3.3 IF-FHN Model

The IF model is the simplest neuron model which mimics certain properties of a biological neuron and is linear before resetting. A slightly more complex model is the IF-FHN model, an IF model but with a nonlinear leakage coefficient, as in a biophysical model. In terms of the output signal-to-noise ratio, we know that the IF and IF-FHN model behave in totally opposite ways when they receive correlated inputs (see [6] for a

discrimination capability of the model neuron. Furthermore, the fraction of coherent inputs which ensures a perfect discrimination is less than that of the IF model. For example, in Fig. 8, with $p_c/p = 25/300$ of coherent inputs the histograms of efferent frequency are well separated when $r = 1$.

4

and denote

$$\alpha(\lambda_1, \lambda_2, c, r) = \{p_c : R_{\min}(\lambda_2) = R_{\max}(\lambda_1)\} \tag{4.1}$$

If it is clear from the context about the dependence of $\alpha(\lambda_1, \lambda_2, c, r)$ on c, r, we sometimes simply write $\alpha(\lambda_1, \lambda_2, c, r)$ as $\alpha(\lambda_1, \lambda_2)$. Hence for fixed (λ_1, λ_2), $\alpha(\lambda_1, \lambda_2)$ gives us the critical value of p_c: when p_c ▪ $\alpha(\lambda_1, \lambda_2)$ the input patterns are perfectly separable in the sense that the the output firing rate histograms are not mixed with TPM=0; when $p_c <$

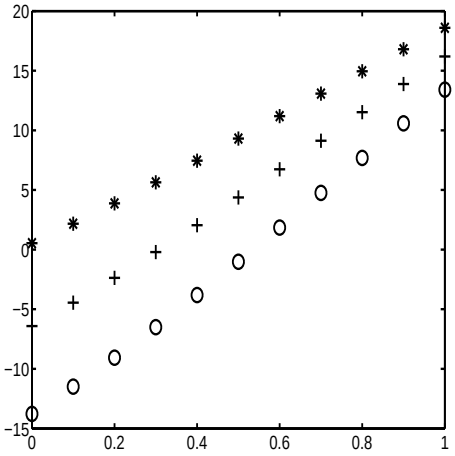
20
15
10
5
0
−5
−10
−15
0
0.2
0.4
0.6
0.8
1

Hence the derivative of the second term in Eq. (4.6) is

$$\frac{2}{L}\cdot\int_0^{V_{thre}L} g'\left(\frac{y-a[p_c\lambda_j+x](1-r)}{a\sqrt{[\lambda_j p_c(1+c(p_c-1))+x](1+r)}}\right) \cdot\frac{-2a(1-r)[\lambda_j p_c(1+c(p_c-1))+x](1+r)-(y-a[p_c\lambda_j+x](1-r)(1+r)}{2a(\sqrt{[\lambda_j p_c(1+c(p_c-1))+x](1+r)})^3}dy$$

$\leq \quad g$

- The output firing rate is an increasing function of inputs
- Input firing rate is confined within a finite region, which is of course the case in neuroscience

we simplify our task from finding out the variance of $\langle T \rangle$ to solving an algebra equation defined in Theorem 1. Theorem 1 is the starting point of all following results.

Theorem 2 *When* $c = 0$ *e have*

$$\alpha(\lambda_1, \lambda_2, 0, r) = \frac{p\lambda_{\max}}{\lambda_2 - \lambda_1 + \lambda_{\max}}$$

independent of r. *When* $c \neq 0$ *e have*

$$\alpha(\lambda_1, \lambda_2, c, r_2) < \alpha(\lambda_1, \lambda_2, c, r_1) < \alpha(\lambda_1, \lambda_2, 0, r) \tag{4.10}$$

here $1 \geq r_2 \neq r_1 \neq 0$ *and furthermore*

$$\alpha(\lambda_1, \lambda_2, c, 1) = \frac{\sqrt{[(\lambda_2 - \lambda_1)(1-c) + \lambda_{max}]^2 + 4p\lambda_{\max}c(\lambda_2 - \lambda_1)} - (\lambda_2 - \lambda_1)(1-c) - \lambda_{\max}}{2c(\lambda_2 - \lambda_1)} \tag{4.11}$$

Before proving the conclusions, we first discuss the meaning of Theorem 2. The first conclusion tells us that with $c = 0$, no matter how strong the inhibitory inputs are, the critical value of p_c is independent of r. In other words, without correlated inputs, increasing inhibitory inputs does not enhance the discrimination capacity of the neuron. In Theorem 3 below, we will further prove that without correlated inputs, if the inputs are separable, so are the outputs and vise versa. The second conclusion says that the discrimination capacity of the neuron is improved if the neuron received correlated inputs. With correlated inputs, increasing inhibitory inputs does enhance the discrimination capacity of the neuron. In particular, we see that for a fixed $c \neq 0$, the optimal discrimination capacity is attained when $r = 1$. Hence Theorem 2 confirms our numerical results on the IF model presented in the previous section.

In Fig. 11 some numerical results of $\alpha(\lambda_1, \lambda_2)$ are shown. It is easily seen that when $c = 0$, $\alpha(\lambda_1, \lambda_2)$ is independent of r.

We want to point out another amazing fact from Theorem 2. $\alpha(\lambda_1, \lambda_2, 0, r)$ and $\alpha(\lambda_1, \lambda_2, c, 1)$ with $c \neq 0$ are both independent of a, V_{thre}, L. When $r = 1, c = 0.1, \lambda_1 =$ 25 Hz, $\lambda_2 = 75$ Hz and $\lambda_{\max} = 100$ Hz and $p = 100$, we have $\alpha(25, 75, 0.1, 1) = 32.5133, \alpha(25, 75, 0, 1) = 66.6667$ (see Fig. 10 and 11). Hence we conclude $32.5133 < \alpha(25, 75, 0.1, r) < 66.6667$ for $r \in (0, 1)$.

Finally we are in the position to answer one of the questions raised in the introduction: a large CV implies a small $\alpha(\lambda_1, \lambda_2, c, r)$. Note that the CV of interspike intervals is the the variance when we calculate the mean interspike intervals. In other words, for each fixed realization of $\xi_i, i = 1, \cdots, p - p_c$, it is the variation of T. When we calculate $\alpha(\lambda_1, \lambda_2, c, r)$, the variance of firing rates histogram is mainly introduced via the masking 'noise'. In other words it is the variation of $\langle T \rangle$. Therefore these are different sources of noise. By increasing the number of interspik intervals, we can reduce the variance of the first kind. Note that in the previous section, we deliberately employ a small number of spikes (100), which might close to the biological reality, to estimate $\langle T \rangle$. The second kind of variance is due to the fluctuation of input signals, or masking noise. In conclusion, increasing inhibitory inputs introduces more variations when we calculate $\langle T \rangle$, but improves neuronal discrimination capacity.

4.2 Input-Output Relationship

In the previous subsections, we only consider the output firing rate histograms. It is certainly interesting to compare the input histograms with output histograms. As before, let Λ be the set of input frequency of the model. For a fixed $(\lambda_1 \in \Lambda, \lambda_2 \in \Lambda)$ with $\lambda_1 < \lambda_2$ we have corresponding two histograms $p_1^i(\lambda)$ and $p_2^i(\lambda)$ of input firing rates, i.e. $p_1^i(\lambda)$we i.e.

$p_c\lambda_2 + \sum_{i=1}^{p-p_c} \xi_i$. Define

$$R^i_{\min}(\lambda_2) = \min\{\lambda, p^i_2(\lambda) \blacksquare 0\}$$

and

$$R^i_{\max}(\lambda_1) = \max\{\lambda, p^i_1(\lambda) \blacksquare 0\}$$

Then the relationship between $R^i_{\min}(\lambda_2) - R^i_{\max}(\lambda_1)$ and $R_{\min}(\lambda_2) - R_{\max}(\lambda_1)$ characterizes the input-output relationship of neuron signal transformations.

We first want to assess that whether $R_{\min}(\lambda_2) - R_{\max}(\lambda_1) \blacksquare 0$ even when $R^i_{\min}(\lambda_2) - R^i_{\max}(\lambda_1) < 0$, i.e. the input signal is mixed, but the output signal is separated. In Fig. 12, we plot $R_{\min}(\lambda_2) - R_{\max}(\lambda_1)$ vs $R^i_{\min}(\lambda_2) - R^i_{\max}(\lambda_1) = \lambda_2 p_c - \lambda_1 p_c - \lambda_{max}(p - p_c)$, which is a function of p_c. It is easily seen that after neuronal transformation, mixed signals are better separated when $c \blacksquare 0$. For example, when $c = 0.1, r = 1$ and $R^i_{\min}(\lambda_2) - R^i_{\max}(\lambda_1) = -5000$ Hz (mixed), but $R_{\min}(\lambda_2) - R_{\max}(\lambda_1) \blacksquare 0$ (separated). The conclusion is not true for $c = 0$, but the separation is not worse after neuronal transformation.

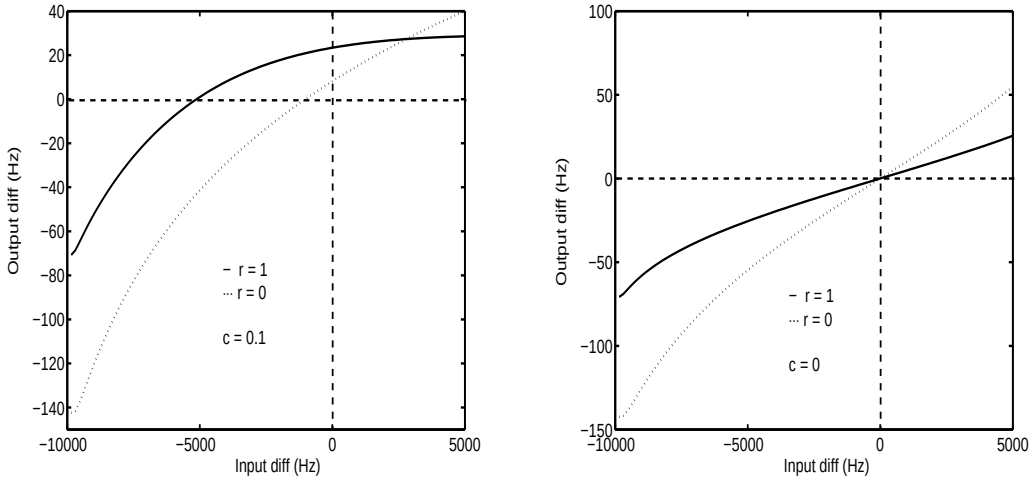

Figure 12: $R_{\min}(\lambda_2) - R_{\max}(\lambda_1)$ vs $R^i_{\min}(\lambda_2) - R^i_{\max}(\lambda_1)$ which is a function of p_c, for $c = 0$ (right) and $c = 0.1$ (left).

Theorem 3 *If* $c \neq 0$ *e have*

$$R_{\min}(\lambda_2) - R_{\max}(\lambda_1) \neq 0 \qquad hen \qquad R^i_{\min}(\lambda_2) - R^i_{\max}(\lambda_1) = 0$$

Proof According to the definition of $R^i_{\min}(\lambda_2)$ and $R^i_{\max}(\lambda_1)$ we have $R^i_{\min}(\lambda_2) = p_c\lambda_2$ and $R^i_{\max}(\lambda_1) = p_c\lambda_1 + \lambda_{\max}(p - p_c)$. From the proof of Theorem 1 we conclude that

$$R_{\min}(\lambda_2) - R_{\max}(\lambda_1) = 0 \qquad \text{when} \qquad R^i_{\min}(\lambda_2) - R^i_{\max}(\lambda_1) = 0$$

if $c = 0$. For $c \neq 0$, it is readily seen that $R_{\min}(\lambda_2) - R_{\max}(\lambda_1) \neq 0$ if and only if

$$\int_0^{V_{thre}L} \left[g\left(\frac{y - a[p_c\lambda_1 + (p - p_c)\lambda_{\max}](1-r)}{a\sqrt{[\lambda_1 p_c(1 + c(p_c - 1)) + (p - p_c)\lambda_{\max}](1+r)}} \right) - \frac{\sqrt{[\lambda_1 p_c(1 + c(p_c - 1)) + (p - p_c)\lambda_{\max}]}}{\sqrt{[\lambda_2 p_c(1 + c(p_c - 1))]}} \cdot g\left(\frac{y - a[p_c\lambda_2](1-r)}{a\sqrt{[\lambda_2 p_c(1 + c(p_c - 1))](1+r)}} \right) \right] dy \tag{4.17}$$

is greater than zero. Since $p_c\lambda_2 = p_c\lambda_1 + \lambda_{\max}(p - p_c)$ we can rewrite Eq. (4.17) as follows

$$\int_0^{V_{thre}L} \left[g\left(\frac{y - a[p_c\lambda_2](1-r)}{a\sqrt{[\lambda_1 p_c c(p_c - 1)) + p_c\lambda_2](1+r)}} \right) - \frac{\sqrt{[\lambda_1 p_c c(p_c - 1)) + \lambda_2 p_c]}}{\sqrt{[\lambda_2 p_c(1 + c(p_c - 1))]}} \cdot g\left(\frac{y - a[p_c\lambda_2](1-r)}{a\sqrt{[\lambda_2 p_c(1 + c(p_c - 1))](1+r)}} \right) \right] dy \tag{4.18}$$

Again from the proof of Theorem 1 we know that g is an increasing function, by noting $\sqrt{[\lambda_1 p_c c(p_c - 1)) + p_c\lambda_2]} < \sqrt{[\lambda_2 p_c(1 + c(p_c - 1))]}$ we conclude that Eq. (4.18) $\neq 0$.

Furthermore, the output difference of firing rates is an increasing function of p_c, this, together with the conclusions above, also implies the remaining results of Theorem 2.

Theorem 3 reveals one of the interesting properties of neuronal transformation. Under the assumption

5 Discussion

We have considered the problem of discriminating between input signals in terms of an observation of efferent spike trains of single neuron. We have demonstrated, both theoretically and numerically, that two key mechanisms to enhance the discrimination capability of the model neuron is to increase inhibitory inputs and correlated inputs. In [10], the authors have theoretically considered discrimination tasks as well. Nevertheless, our approach is very different from theirs. We have concentrated on neuronal mechanisms, but their results are more or less a direct application of results in statistics.

There are many issues to be further explored in the future.

- We have only considered to accomplish the discriminating task and have not included time constrains. Definitely it is of vital importance for a neuronal system to tell one signal from the other within a time window as short as possible.
- We have tested our model with static inputs. It is an interesting question to generalize our results here to time-varying inputs as reported in [15]. Such a study might be helpful to clarify the ongoing debate on the advantages of 'dynamical stimuli' over the 'static stimuli'.
- The input signal used here is very naive. To transform the image of moving dots to input signals specified in the present paper requires a neural network to preprocess the image. Hence to devise a network model (spiking neural networks or Reichardt detector [3]) to reproduce our results is one of our ongoing research topics. We expect that such a study could provide us with a template to compare

Discriminating between different input signals is probably more fundamental constrains on the neural system than others such as maximizing input-output information or redundancy reductions, a view recently echoed in [1]. To understand it will reveal principles employed by neuronal systems which remain mysterious to us. The issue discussed here is currently a hot topic in neuroscience (for example see [13]). Our approach provides us with a solid theoretical foundation for further study and we expect that our approach also opens up many interesting questions to be further investigated in the future.

Acknowledgement. Partially supported by a grant from EPSRC(GR/R54569), a grant of the Royal Society and an exchange grant between UK and China of the Royal Society. F. Liu acknowledges the support from NNSF of China 30070208.

References

[1] Barlow H. (2001) Redundancy reduction revisited. *Net ork* **12** 241-254.

[2] Britten K.H., Shadlen M.N., Newsome, W.T., Celebrini S., and Movshon J.A. (1992) The analysis of visual motion: a comparison of neuronal and psychophysical performance. *J. Neurosci.* **12** 4745-4765.

[3] Borst A. (2000) Models of motion detection. *Nature Neuroscience* **3** 1168-1168.

[4] Brown D., Feng J., and Feerick, S. (1999) Variability of firing of Hodgkin-Huxley and FitzHugh-Nagumo neurons with stochastic synaptic input. *Phys. Rev. Letts.* **82**, 4731-4734.

[5] Feng, J.(1997) Behaviours of spike output jitter in the integrate-and-fire model. *Phys. Rev. Lett.* **79** 4505-4508.

[6] Feng J. (2001) Is the integrate-and-fire model good enough? –a review. *Neural Net orks* **14** 955-975.

[7] Feng J. (with G. Leng et al.) (2001) Responses of magnocellular neurons to osmotic stimulation involves co-activation of excitatory and inhibitory input: an experimental and theoretical analysis. *J. Neurosci.* **21** 6967-6977.

[8] Gammaitoni L., Hänggi P., Jung P. and Marchesoni F. (1998) Stochastic resonance. *Revie s of Modern Physics* **70** 224-287.

[9] Grossberg, S, Maass W., and Markram H. (2001) Neural Networks (Special Issue), vol. **14**.

[10] Gold J.I., and, Shadlen M.N. (2001) Neural computations that underlie decisions about sensory stimuli. *Trends In Cognitive Sciences* **5** 10-16.

[11] Hopfield J.J., and Brody C.D. (2000) What is a moment? 'Cortical' sensory integration over a brief interval. *Proc. Natl. Acad. Sci. USA* **97** 13919-13924.

[12] Hopfield J.J., and Brody C.D. (2001) What is a moment? Transient synchrony as a collective mechanism for spatiotemporal integration. *Proc. Natl. Acad. Sci. USA* **98** 1282-1287.

[13] Kast B. (2001) Decisions, decisions ... *Nature* **411** 126-128.

[14] Parker A.J., and Newsome W.T. (1998) Sense and the single

.78(dern).21(a)6967-6977(sensory)Te

[19] Tuckwell H. C. (1988) *Introduction to Theoretical Neurobiology* Vol 2, Cambridge University Press.

[20] van Vereeswijk C., Abbott L.F., and Ermentrout G.B. (1994) When inhibition not excitation synchronizes neural firing. *Jour. Computat. Neurosci.* **1** 313-321.

[21] Zohary E., Shadlen M.N., and Newsome W.T. (1994) Correlated neuronal discharge rate and its implications for psychophysical performance. *Nature* **370** 140-143.